2018

Organic Contaminant Removal Efficiency of Sodium Bentonite/clay (BC) Mixtures in High Permeability Regions Utilizing Reclaimed Wastewater: A meso-scale study

Yang Xiao

Recommended Citation

Xiao, Y., Li, YK. & Ning, ZG. (2018). Organic Contaminant Removal Efficiency of Sodium Bentonite/clay (BC) Mixtures in High Permeability Regions Utilizing Reclaimed Wastewater: A meso-scale study. *Journal of Contaminant Hydrology*, vol. 210, pg. 1-14. doi:10.1016/j.jconhyd.2018.01.008

Organic contaminant removal efficiency of sodium bentonite/clay (BC) mixtures in high permeability regions utilizing reclaimed wastewater: A meso-scale study

Abstract

Wastewater reclamation now represents an effective measure for sustainable water resource management in arid regions, however wastewater components (organic micropollutants) may potentially impact local ecological and/or human health. Previous studies have shown that sodium bentonite/natural clay (BC) mixes may be used to effectively reduce riverbed infiltration in regions characterised by excessively high hydraulic conductivity. Accordingly, the current study sought to investigate the contaminant removal efficiency (*Re*) of several BC mass ratios in simulated dry riverbeds. Results indicate that the measured *Re* of NH_4^+-N, COD_{cr} and BOD_5 increased in concurrence with an increasing sodium bentonite ratio, up to a maximum *Re* of 97.4% (NH_4^+-N), 55.2% (COD_{cr}), and 51.5% (BOD_5). The primary contaminant removal site was shown to be the infiltration-reducing (BC) layer, accounting for approximately 40%, 60%, and 70% of NH_4^+-N, COD_{cr} and BOD_5 removal, respectively. Conversely, the removal efficiency of NO_3-N was found to be low (<15%), while total phosphorous (TP) was found to actively leach from the infiltration-reduction layer, resulting in measured TP discharges 2.4-4.8 times those of initial infiltration values. The current study provides a technical baseline for the efficacy of sodium bentonite as an effective bi-functional material in areas utilizing reclaimed water i.e. concurrent reduction of infiltration rates (Function 1) and decontamination of reclaimed wastewater infiltration/recharge (Function 2). Findings indicate that sodium bentonite-clay mixes may represent a feasible alternative for managing recharge of non-potable aquifers with reclaimed wastewater.

Key words: infiltration, reclaimed water, bentonite, clay, groundwater pollution, contaminant removal

1. Introduction

Over recent decades, China, along with other economically and climactically similar regions, has faced significantly increasing water requirements, resulting in groundwater overuse, decreasing watertables, and increasing surface water infiltration rates (Foster & Chilton, 2003; Dong *et al.*, 2012). Increasing urbanisation has resulted in parallel increases in wastewater production, thus, it is considered that reclaimed wastewater reuse now represents a potentially effective and increasingly employed solution to resolving the global problem of spatial and temporal water shortages, in addition to reducing effluent discharges to aquatic environments, and thus improving ecological health (Bischel *et al.*, 2013; Chhipi-Shrestha *et al.*, 2017). China is currently the largest global user of reclaimed wastewater (Yi *et al.*, 2011). However, the inherent nature of reclaimed wastewater (i.e. high levels of organic compounds, including nitrogen, phosphorous, and chemical/biochemical oxygen demand), in concurrence with increasing infiltration rates due to climate change, subsequently leading to decreased subsurface retention and natural attenuation, has resulted in elevated contamination risks to local aquifers and wells (Rose, 2007; Li *et al.*, 2012; Bischel *et al.*, 2013; Chhipi-Shrestha *et al.*, 2017). Previous studies have shown that via a series of physical, chemical and biological mechanisms, contaminants in percolating recharge water may be removed by riverbed media (Drzyzga & Blotevogel, 1997; Rauch-Williams & Drewes, 2006; Kumar *et al.*, 2016). The elevated cation exchange capacity (CEC) of bentonite clays and other pillared forms of bentonite result in a high contaminant adsorption capacity; previous studies have shown bentonite to be an effective solid adsorption media with respect to iron nanoparticles (Shi *et al.*, 2011), phosphates (Haghseresht *et al.*, 2009), ammonia (Zhou *et al.*, 2015) and amoxicillin (Putra *et al.*, 2009). These purification effects are intrinsically associated with media lithology, hydraulic residence time, and microbial community composition (Shuang, 2008; Liu & Wang, 2009; Wu, 2009). For example, typically elevated levels of microbial activity during the warmer summer months has been shown to increase subsurface nitrate removal (Grischek *et al.*, 1998), while Yu *et al.* (2011) have recently shown that "self-purification capacity" improves in parallel with increased hydraulic retention. However, riverbed media structure, microbial community structure and dynamics, and potentially influential external conditions represent complicated independent systems and processes, made all the more complex via environmental interaction (Fierer *et al.*, 2003; Lu *et al.*, 2006).

Sodium bentonite has been characterized by high physical and chemical stability (Bakandritsos *et al.*, 2004; Klika *et al.*, 2007), with the cycling of both matter and energy between the water and riverbed sediment remaining unchanged after material placement (Baoliang, 2009; Zhang & Jia, 2010). For example, while numerous infiltration reduction measures are available and provide high levels of impermeability (geo-membranes, masonry), they have also been shown to damage necessary ecological relationships between the aqueous, soil, gaseous and bio- phases. Thus, it may be an effective soil treatment for simultaneous recharge decontamination and infiltration regulation, however, to what depth and magnitude self-purification occurs in the subsurface remains unknown and thus requires further

investigation.

Accordingly, the current study is the first to examine the decontamination effects attributable to installed sodium bentonite infiltration reducing layers in areas utilising reclaimed water. The authors consider that meso-scale experiments offer several advantages over small-scale experiments and in-situ field testing e.g. in-situ field testing may introduce levels of natural uncertainty and variability via external factors. Based upon the developed experimental soil column and multi-apperture lysimeter (hereafter referred to as nodes) approach, this study investigated the purification effects of sodium bentonite mixtures with respect to organic contaminants, and how this effect varied with simulated riverbed depth. Findings provide an effective theoretical basis for groundwater impact assessment with respect to reusing reclaimed water in regions characterized by excessively high infiltration rates and/or vulnerable groundwater systems. Additionally, results may be used to examine the efficacy of sodium bentonite/clay mixtures as a bi-functional material for parallel infiltration reduction and recharge purification.

2. Methodology

2.1 *Experimental Apparatus and Procedures*

2.1.1 Experimental Apparatus

The current study formed part of a larger overall project which sought to elucidate the effects of sodium bentonite-clay mixtures on riverbed infiltration of reclaimed wastewater. Six 500mm (inner diameter) poly-methyl methacrylate (PMMA) simulation columns were used for data collection, with one column employed for each treatment approach (n = 4), and one used for each experimental control (n = 2). All experimental testing was undertaken in the absence of sunshine and external heat sources, with constant hydraulic head maintained to appropriately mirror natural riverbed conditions. The developed experimental apparatus comprised four component systems, namely, i) a support system (steel supporting frame and base), ii) a water supply system (including a 5000L storage tank, water supply pipeline (ID 20mm), water pump, and 60L Mariotte bottle), iii) the principal soil column simulation system (3000 x 500mm (ID) PMMA column and tensiometers), and iv) a sampling system (PVC protection box, soil water and groundwater (discharge) sampling vessels) (Figure 1a). Due to the relatively large depth of mesoscale experimental soil columns (2000mm) compared with previous bench-scale experiments (Zhou *et al*., 2015), extended breakthrough times from infiltration to discharge were expected and subsequently encountered. Accordingly, the discharge concentration was found to lag relative to the infiltration concentration, therefore a multi-apperture lysimeter (bore diameter, d = 25mm) approach was employed to examine the effects of subsurface depth on contaminant concentrations, and more appropriately simulate and elucidate "real world" conditions. The multi-apperture lysimeter (bore diameter, d = 25mm) approach was taken via in-situ soil water and discharge sample collection at six design depths (h1 = 200mm, h2 = 600mm, h3 = 1000mm, h4 = 1400mm, h5 = 1800mm, and h6 (discharge) = 2000mm). Lysimeters were constructed of porous clay piping, with discharge samples (2000mm) collected via a drainage valve at the bottom of each experimental column.

Simulation columns were filled (i.e. "bottom up") as follows (Figure 1): A 350mm thick "supporting layer" (<2mm quartz sand (50mm thickness) AND <20mm gravel (100mm thickness) AND ⩾20mm gravel (200mm thickness)) → 2000mm riverbed media →the "Experimental" (infiltration reduction) layer → A 50mm "Protective" layer (20mm layer of <2mm quartz sand, AND 30mm of <20mm gravel). The "protective layer" was employed to minimize disturbance of the experimental layer during and after reclaimed wastewater addition, and was placed in direct contact with experimental materials. The supporting layer provided a robust foundation/framework for the materials above and comprised ≈200mm of washed gravel. An excess (static) water level was not maintained at the top of experimental columns at all times; in order to simulate real world conditions, seeding of wastewater represented periodic "events", subsequently creating variable, dynamic levels of saturation in the subsurface throughout the experimental period.

Riverbed media (RM) were filled in tamped 70-80mm layers to ensure uniform moisture ratio, soil dry density and soil volume prior to experimental initiation. To avoid preferential laminar flow between layers, layer surfaces were abraded prior to filling in the subsequent layer. Preliminary bench-scale experiments (Zhou *et al.*, 2015) resulted in the use of a 200-mesh chinlon sheet being positioned directly on the final riverbed media layer, followed by application of a 20mm BC (treatment) layer. Based upon results of osmotic coefficient (K_s) pre-experiments (Data not presented here), and to avoid particle disturbance, a 60mm RM layer was employed.

2.1.2. Experimental Treatments and Controls

Six experimental subsets were examined, including four experimental treatment groups (BC12, BC16, BC16-600, and BC20) and two control treatment groups (RM and CK) (Table 1). Based upon results of a previous bench-scale study (Zhou *et al.*, 2015), BC treatment mixture ratios of 12% bentonite + 88% clay (BC12), 16% bentonite + 84% clay (BC16), and 20% bentonite + 80% clay (BC20) were employed as experimental treatments, with these experiments carried out at a constant hydraulic head height of 300mm. To investigate the potential influence of fluctuating hydraulic head (water level) on contaminant removal efficiency, an analogous experiment was carried out for BC16 at 600mm hydraulic head height (BC16-600). Natural river mud's have been found to act as natural infiltration reduction materials (Li *et al.*, 2012), and were thus included in the current study for comparative purposes (Table 2). Finally, the remaining control column (CK) was filled with natural clays and characterized by an absence of any additional treatment which could potentially (positively or negatively) influence infiltration rates.

2.1.3. Experimental Materials

Natural sodium bentonite was acquired from the Xuanhua bentonite mine (Miyun Yunfeng Earth and Stone Plant) in the Miyun prefecture, while natural clays were sourced from the Yan Village Soil Plant in the Mentougou district (CK), Beijing. Riverbed media (RM) was taken from the dry riverbed at Zhongmen Temple Channel at a sampling depth range of 1-3m. The sampling location is immediately downstream from the Yongding River and is equivalent to the larger river in terms of media type, depth and stratification. Large particles were removed by sieving (2cm). River mud was sampled from Lianshi Lake, which is located on the Yongding River. The primary physical characteristics of treatment materials (particle size distribution, initial moisture content and dry weight) were analysed via sieving (GB/T 21524-2008) and oven drying (ASTM D2216), respectively (Table 3).

2.1.4. Sampling Frequency

Initially, sampling in the BC and RM columns was undertaken every 3 days over a 30-day period, followed by sampling every 7 days over a 56-day period, sampling every 15 days over a 30-day period and finally, monthly sampling (30-day) for the remainder of the experimental period (8 months). In the

untreated control column (CK), due to significantly shorter breakthrough times acquired from the first study phase, soil water was collected 3, 5, 10, 15, and 20 hours following introduction of reclaimed wastewater (Table 4).

2.2 Reclaimed wastewater and soil water/discharge quality

Reclaimed water used in experiments was acquired from the Qinghe Reclaimed Water Treatment Plant, with discharges conforming to current Chinese standards for environmental usage (GB/T18921-2002(II) – Urban Water Consumption); this facility employs the Anaerobic-Anoxic-OXic (ANANOX) wastewater recycling process and currently supplies approximately 80,000 m^3/d to Olympic Lake (159,000 m^3) in the Chaoyang district of Beijing. Reclaimed water quality was periodically evaluated during the experimental period (n = 28); in addition to pH, the following water quality parameters were monitored: chemical oxygen demand (CODcr), biochemical oxygen demand ($BOD_{5)}$, total nitrogen (TN), ammonia (NH_4^+-N), nitrate (NO_3^-N), total phosphorus (TP). Pre-experimental reclaimed water quality results are presented in Figure 2. Soilwater and discharge samples were analyzed at a certified laboratory, with all analytical techniques confirming to Chinese Regulations (Table 5).

2.3 Calculation of Contaminant Removal Efficiency (R_e)

Due to the relatively large depth of the mesoscale experimental soil columns (2000mm), extended breakthrough times from infiltration to discharge were encountered, resulting in marked hysteresis i.e. a significant difference between soil water content and soil water potential during the wetting/drying process (O'Kane & Flynn, 2007). Subsequently, measured infiltration quality was not constant, thus contaminant concentration has been employed throughout the current study to calculate removal efficiency (R_e). This approach necessitated several analytical assumptions, outlined below.

2.3.1 Analytical Assumptions

i. Constant storage within soil column

Based upon the expectation of steady state conditions within the soil columns and per the principle of conservation of matter, it was assumed that over the duration of a specific period, the volume of water within soil columns remained in equilibrium i.e. infiltration volume equal to discharge volume.

ii. Volumetric variations associated with solid-phase (residual) contaminants were negligible

Measured variations between initial (pre-experimental) and 1-year contaminant concentrations are presented in Tables 6 and 7. In comparison with the concentrations of aqueous-phase (infiltration) contaminants, variation in the concentrations (and thus ratio) of solid-phase contaminants (i.e. residual contaminants associated with the surface of riverbed media and infiltration reduction materials) was typically small (<1%). Accordingly, only the R_e of aqueous-phase contaminants were examined, as it was

considered that no significant leaching of residual contaminants likely occurred during the experimental period.

iii. Stable short-term removal efficiencies

Due to the prolonged experimental duration and decreasing sampling periodicity, numerous batches of reclaimed water were employed, thus resulting in slight variations in infiltration (inflow) quality, and therefore by extension, discharge quality. Therefore, it was assumed that R_e remained stable and linear over short (i.e. 10-14 day) periods i.e. the ratio between discharge concentration and infiltration concentration was represented by a constant value over these periods.

2.3.2 Aqueous-phase contaminant concentrations

By dividing the discharge and infiltration periods (T_i) according to measured water volume and contaminant concentration, the contaminant concentration during each period may be ascertained, permitting calculation of the total contaminant volume (amount) (S) (Figure 3). Based upon outlined assumptions, the following parameters were obtained:

i. Discharge concentration at a "transient point" ($C_{k2\ OUT}$):

Discharge contaminant concentration varied considerably throughout the experimental period, thus in order to acquire accurate *Re* measurements, frequent process outflow monitoring was necessary. Discharge concentrations were measured at nodes L_3 and L_4 (Figure 3). Variation of inflow (Node K_1) water quality caused a time-lagged outflow (Node K_2) variation (with the same being true between L_1 and L_2). Due to the increased time periods between sampling events associated with later experimental phases, it was be expected that proportionality associated with this correlation (K_1, K_2) would not be accurately reflected at Node K_2. To calculate the concentration at Node K_2, it was assumed that short-term removal efficiencies remained stable, with the discharge concentration at Node K_2 represented by:

$$C_{k_2 OUT} = \frac{C_{k_1 IN}}{C_{l_1 IN}} * C_{l_3 OUT} \qquad \textit{(Eqn. 1)}$$

where $C_{k2\ OUT}$, $C_{k1\ IN}$, $C_{l1\ IN}$ and $C_{l3\ OUT}$ are the infiltration (IN) or discharge (OUT) concentrations specific nodes.

ii. Discharge concentration of a calculated discharge period ($C_{i\ OUT}$):

$$C_{iOUT} = \frac{C_{(k-1)OUT} + C_{kOUT}}{2} \qquad \textit{(Eqn. 2)}$$

where $C_{i\ OUT}$ is the discharge concentration in the specified period *I*, and $C_{(k-1)OUT}$ and $C_{k\ OUT}$ represents the discharge concentration at a specific node.

iii. Discharge concentration over a specified infiltration period ($C_{i\ IN}$):

The infiltration period between adjacent detection nodes (i.e. time taken for wastewater to flow downwards from one node to the next (deeper) node) was used to calculate total contaminant volume. For contaminant mass calculations, nodes were reset in concurrence with the introduction of new inflow (waste)water, with the adjacent detection node used as the calculation period (i.e. infiltration concentration is equal to the former node concentration). If the selected calculation period contained multiple detection nodes, based upon the duration attributed to each node, the weighted average method was used to calculate the infiltration concentration, as follows:

$$C_{iIN} = \frac{C_{(k-1)IN} d_{k-1} + C_{kIN} d_k + \ldots C_{lIN} d_l}{d_{k-1} + d_k + \ldots d_l} \qquad \textit{(Eqn. 3)}$$

where $C_{i\ IN}$ is the discharge concentration during specified period (*I*), $C_{(k-1)IN}$, $C_{k\ IN}$ and $C_{l\ IN}$ represent infiltration concentrations at specific nodes, and d_{k-1}, d_k and d_l refer to the duration of the corresponding infiltration concentration period.

iv. Cumulative infiltration (W_i):

Based upon measured volumetric changes in the Markov bottle, cumulative infiltration was calculated as:

$$W_i = F(t_k) - F(t_{k-1}) \qquad \textit{(Eqn. 4)}$$

where W_i represents cumulative infiltration during period *I*, and $F(t_k)$ and $F(t_{k-1})$ signify cumulative infiltration at nodes *k* and *k-1*, respectively.

v. Total contaminant concentration in aqueous phase (S_W):

$$S_i = C_i W_i \qquad \textit{(Eqn. 5)}$$

$$S_W = \sum_{1}^{n} T_i \qquad (Eqn.\ 6)$$

where S_i refers to the total contaminant concentration during period i and S_W represents the total contaminant volume measured over the 290 day experimental period.

v. Contaminant removal efficiency (Re):

$$Re = \frac{T_{W_{IN}} - T_{W_{OUT}}}{T_{W_{IN}}} \times 100\% \qquad (Eqn.\ 7)$$

where T_{Win} and T_{Wout} represent the total (aqueous phase) contaminant volumes of infiltration and discharge, respectively.

3. Results

The primary objective of the CK column experiment was acquisition of evidence-based background contamination values. Upon calculation of CK R_e and comparison with the total volume of inflow contaminants, negligible variation (<1%) was found between contaminant concentrations in the solid phase (i.e. contaminants on soils/sorbent materials including riverbed media and infiltration reduction material (BC) samples but not including particles suspended in the aqueous phase), thus only aqueous phase contaminant R_e is considered here. Unless specified, all calculated R_e values refer to a 2000mm riverbed depth over the duration of the experimental period.

3.1 Ammonium (NH_4^+-N) Removal

As shown (Figure 4), all treatment groups (BC12, BC16, and BC20) exhibited a high level of NH_4^+-N removal; sodium bentonite fractions of 12, 16 and 20% were associated with final NH_4^+-N discharge concentrations in the ranges 0.01–1.61 (*Re* = 81.2%), 0.01–0.25 (*Re* = 85.6%) and 0.01–0.19 mg/L (*Re* = 97.4%), respectively. Thus, decreased NH_4^+-N discharge concentrations concurred with an increasing BC ratio; discharge concentrations associated with both BC16 and BC20 complied with current Chinese Groundwater Quality Standard Level III (GB/T14848-93).

Similarly, discharge concentrations from the RM column complied with Groundwater Quality Standard III, falling within a measured range of 0.01 to 0.19 mg/L NH_4^+-N (*Re* = 95.3%). As the sodium bentonite content increased from 12% to 20%, NH_4^+-N *Re* increased by 16.2%, representing a statistically significant between (treatment) groups difference (t = -7.650, p = 0.001). While an increased (300mm) pressure head was found to influence *Re* (+7%), this increase was not statistically significant at the 95%

level (BC16 vs BC16-600; t = 1.282, p = 0.256). Analyses indicate an increasing *Re* in concurrence with increased riverbed media depth for BC12, BC16 and BC16-600. For example, calculated *Re* at 2000mm depth (i.e. discharge) were 41.3% and 40.0% higher than at 200mm depth in the BC12 and BC16 columns, respectively (Figure 4). Conversely, >90% of the final *Re* was achieved at a depth $\leqslant$200mm in both the BC20 and RM columns, thus highlighting the primary NH_4^+-N removal site.

3.2 Nitrate (NO_3^-N) Removal

As shown (Figure 5), NO_3^-N removal exhibited by all treatment groups was low. BC-12, BC-16, and BC-20 were associated with NO_3^-N discharge concentrations occurring with the ranges 10.4–47.8, 6.42–45, and 8.21–50.4 mg/L, respectively, all of which fail to comply with current groundwater quality standards (Level IV). Within the RM column, a maximum measured discharge concentration of 259 mg/L was recorded, with a mean range of 12.6–33.2 mg/L from 20–289 d, equating to compliance with groundwater quality standard Level II.

The calculated *Re* of NO_3^-N in BC-12, BC-16 and BC-20 was 7.2, −3.7 and −7.6%, respectively, thus exhibiting a decreasing *Re* in concurrence with an increasing sodium bentonite content (p = 0.05). The *Re* in RM reached 38.6% during the 20–289d period, thus significantly outperforming all treatment groups. The *Re* in BC16-600 was 0.22%, and thus did not differ significantly from BC16 (p >0.05). Overall, riverbed media depth was not shown to significantly affect the calculated *Re* of NO_3^-N in any treatment groups; all remained at or below 10% throughout the range of experimental media depths. Conversely, the *Re* of NO_3^-N in RM decreased from 72.5 to 0% over the 200–2000 mm depth range.

3.3 Total Nitrogen (TN) Removal

Sodium bentonite ratios of 12, 16, and 20% were associated with TN concentrations in the ranges 11.3–69.5, 25.48–48.9 and 21.0–51.6 mg/L, respectively (Figure 6), primarily due to the existing form of N in experimental reclaimed water being NO_3-N, and thus the Re of TN was similar to NO_3-N as expected. A measured range of 4.84–34.5 mg/L (20–289d) was found in the RM column. The calculated TN *Re* associated with BC12, BC16 and BC20 were 12.2, 4.3 and 4.4%, respectively. The 7.8% mean *Re* difference between BC12 and BC20 was shown to be statistically significant (p <0.05). After 20 days, the calculated *Re* in the RM column was 7.5%, rising to 44.6% after 289 days; thus, the removal efficiency of total nitrogen was 32.4 – 40.3% greater in the RM (control) column than in experimental treatment columns. BC16-600 exhibited a TN *Re* of 5.1% at 2000mm, and thus only outperformed BC16 by 0.8% over the experimental column depth (p >0.05). Measured TN R_e did not vary significantly with riverbed media depth in BC12 and BC16, with no visible or empirical trend found. Conversely, the *Re* of TN in BC20 exhibited a relatively continuous decrease in concurrence with depth i.e. 9.2% between 200 and 2000 mm, while the R_e of TN in RM decreased dramatically from 70.1% (200 mm) to 0% (2000 mm).

3.4 Total Phosphorous (TP) Removal

TP discharge concentration was found to remain elevated in final column discharge (Figure 7). Measured TP discharge concentration ranges of 0.32–1.28, 0.66–1.13 and 0.49–1.12 mg/L were associated with BC-12, BC-16, and BC-20, respectively, with corresponding leaching concentrations found to be approximately 2.4, 3.9, and 4.8 times those of infiltration concentrations. Measured discharge concentrations ranged from 0.02 to 1.6 mg/L in the RM (60mm natural sediment) column, with leaching concentrations 2.8 times those of infiltration concentrations.

Apart from BC12, TP concentrations exhibited an overall increase in concurrence with increasing riverbed depth, approaching its maximum value within all simulation columns at approximately 1400mm, followed by subsequent increases. The calculated R_e associated with BC12 also displayed an overall decrease in concurrence with increasing depth, although it exhibited a greater final R_e ($\approx$13%).

3.5 BOD_5 and CODcr Removal

Measured BOD_5 discharge ranges of 0.5–4.8, 2.00–3.4 and 0.6–2.7 mg/L were associated with BC-12, BC-16, and BC-20, respectively, with calculated BOD_5 R_e 37.5%, 47.5% and 55.2% (Figure 8). Discharge ranges for CODcr were 5.0–24.3, 8.2–18.0, and 7.2–14.8 mg/L for the BC-12, BC-16, and BC-20 infiltration reduction treatments, respectively, with calculated CODcr R_e of 37.8%, 48.6%, and 51.5% (Figure 9). No significant difference was found to exist between the maximum R_e of BOD_5 (51.3%) and CODcr (49.7%) in BC16-600 and those calculated for BC16 (300mm hydraulic head) ($p > 0.05$) i.e. differing hydraulic head height was not found to significantly affect BOD_5 or CODcr removal.

The measured discharge concentrations of BOD_5 and CODcr in the RM column were 1.6–4.6 and 7.2–22.6 mg/L, respectively, with broadly similar calculated removal efficiencies of 43.4% (BOD_5) and 40.9% (CODcr). The maximum calculated R_e of BOD_5 and CODcr in RM were 61.3% and 64.6%, respectively, both of which were noted during the 20–120d period.

Significant fluctuation was noted with respect to riverbed media depth and the calculated R_e of BOD_5 and CODcr in all (treatment and control) soil columns, with no overarching trend identified. For example, the *Re* of BOD_5 and CODcr in BC12 initially increased in concurrence with depth, reaching maximum values at 1400 mm and 1000 mm, respectively, after which a gradual decrease was exhibited. Conversely, in BC20, calculated R_e increased steadily within the 200–1000 mm depth range, followed by a sharp decrease from 1000–1400 mm, after which it increased gradually. Findings indicate that the primary BOD_5 and CODcr removal sites in all columns was in the infiltration-reducing layer. The calculated BOD_5 R_e of BC12, BC16, and BC20 increased with riverbed media depth (200 to 2000 mm) by 10.6%, 5.4% and 12.1%, respectively, with corresponding CODcr R_e increases of 14.4%, 3.3%, and 6.8% over the same depth range. Accordingly, findings show that >70% of BOD_5 removal occurred within the BC treatment layer ($\leqslant$200 mm), with >60% of CODcr removal also taking place within this layer.

4. Discussion

The current study sought to examine the efficacy of sodium bentonite-clay (BC) mixtures for reducing infiltration in high permeability regions, in concurrence with decontamination of recharge derived from reclaimed wastewater. Sodium bentonite is a readily available and inexpensive material, characterised by a large surface area, which in tandem with its positive ionic exchange capacity and adsorptive properties has been shown to influence the transport and removal of contaminants (Putra *et al.*, 2009; Kumar *et al.*, 2016). To date, this represents the first specific investigation of reclaimed wastewater infiltration and decontamination at the meso-scale.

Nitrification and denitrification are the predominant nitrogen removal processes in the subsurface (Hill *et al.*, 2000). Huang *et al.* (2006) have previously employed indoor soil columns for simulating vertical river bank filtration and associated NH_4^+-N percolation, finding a removal efficiency of approximately 87%, with Abel *et al.* (2014) reporting similar results (88-98%) in a 4.2m soil aquifer treatment system. In the current study, all infiltration reducing treatments (BC) exhibited a final NH_4^+-N R_e greater than 80%, with an R_e of >90% found within the upper 200mm soil depth when BC20 was employed, up to a maximum of 97.4% at 2000mm depth. Based upon previous work by Lumbanraja & Evangelou (1994) and Lee *et al.* (2006), current study results indicate that that increasing sodium bentonite contents result in increased NH_4^+-N adsorption within the treatment layer, while aerobic conditions in the unsaturated zone resulted in effective nitrification below the treatment layer i.e. a notable NH_4^+-N R_e increase occurred with depth in both the BC12 and BC16 soil columns. Conversely, Guo & Li (2004) have shown that enhanced NH_4^+-N removal is achievable via a reduction in hydraulic loading. Previous findings indicate that the infiltration-reducing effects of BC20 and RM were higher (Data not presented here), thus significantly impeding the movement of water and NH_4^+-N, and increasing the NH_4^+-N retention time within the infiltration-reducing layer. Accordingly, the *Re* of NH_4^+-N in BC20 and RM was greater than those associated with BC12 and BC16. The riverbed medium employed in the current study was sand, resulting in a reduced hydraulic retention time, thus focusing NH_4^+-N removal within the infiltration-reducing layer.

Kopchynski *et al.* (1996) have previously shown that while NH_4^+-N can be nitrified effectively in most parts of the soil infiltration system, denitrification does not readily occur. For example, Valasquez *et al.* (2016) recently reported an NO_3-N removal rate of 15.17 % via laboratory scale soil aquifer treatment (SAT) of secondary effluents and combined sewer overflows (CSOs) in Ontario, Canada. The denitrification process is a complex one, typically requiring four conditions: (i) presence of nitrogen oxides (e.g. NO_3^-) as electron acceptors (ii) an anaerobic or anoxic environment, (3) presence of a suitable electron donor, and (iv) presence of denitrifying bacteria (An & Gardner, 2002). In the current study, while the first condition was satisfied, it is considered that the underlying riverbed media constituted an aerobic environment, thus inhibiting the formation of nitrate reductase and resulting in low levels of NO_3-N removal (<10%). Due to the necessary experimental conditions that were adhered to as part of this study (e.g. hermetic

seals), it was not possible to directly measure oxygen in the subsurface, thus representing a study limitation. Based upon measured data, all soil columns exhibited as high NH_4^+-N removal efficiency, conversely, NO_3-N removal efficiencies were found to be low. Accordingly, the authors consider that this provides strong evidence of the riverbed media constituting an aerobic environment, as ammonium nitrogen is typically oxidized into nitrates under aerobic condition, with nitrates gradually converted to nitrogen gas under anaerobic conditions.

Organic carbon or reactive metals in the subsurface represent the most frequently available electron donors (Puckett & Cowdery, 2002). In the current study, it is likely that high microbial loading in the reclaimed wastewater resulted depleted levels of dissolved organic carbon (DOC) in the riverbed media. Moreover, as reported by Bate & Spaldin (1998), infiltration processes typically result in oxidation of DOC, with DOC content typically decreasing with depth, thus reducing the occurrence of denitrification. Starr & Gillham (1989) have found that organic carbon is frequently the limiting factor prohibiting denitrification in groundwater environments. The authors consider that the reclaimed water employed in the current study provided an insufficient supply of organic carbon. As shown (Figure 5), NO_3^--N removal in the RM column reached approximately 70%, primarily due to the high initial TOC (48.4g/kg) and TN (4.16g/kg) contents of river mud employed in experiments (Table 2). Accordingly, the C/N ratio within the RM soil column was high enough to provide ample energy for effective denitrification, and particularly at shallower depths (<1000mm). Based upon these findings, it is recommended that further work focus on subsurface organic carbon requirements and sources in areas characterized by high infiltration and reclaimed wastewater use, as these likely represent the primary restriction factors for biological denitrification.

Phosphorus may be removed during soil aquifer treatment/managed infiltration via soil particle adsorption and/or chemical precipitation with ions present in the soil including calcium, magnesium, oxides/hydroxides of iron, and aluminium (Idelovitch *et al*. 2003). Previous studies have reported conflicting results with respect to phosphorus removal from soil aquifer treatment systems. A previous modelling study undertaken by Vanderzalm *et al.* (2013) reports that while TOC and TN removal ranged from 25-40% and 46-87%, respectively, total phosphorous (TP) was subject to reversible removal via adsorption and desorption processes i.e. steady-state results were unobtainable. Conversely, Kanarek & Michail (1996) found that recharge water used for unrestricted irrigation exhibited >90% phosphorus removal after soil aquifer treatment at the Dan region reclamation project in Israel. In the current study, results indicate that phosphorus was actively leached from the infiltration treatment layer (Figure 7), with leaching concentrations found to increase in concurrence with increasing sodium bentonite content. Likewise, TP values were found to increase significantly (x 2.6 times) in the RM soil column. As previously outlined, all analyte concentrations in the untreated control column (CK) apart from those associated with phosphorus were found to continuously decrease over time, thus results indicate that the high background values of phosphorus in riverbed media resulted in significant phosphorus leaching throughout

the experimental treatment phase. Richards *et al*. (2017) recently report that the complex composition of septic tank effluents effectively reduced the absorption ability of untreated soils and soils with reduced microbial activity. It is considered that a similar process may have occurred during the current study, while the presence of other substances in reclaimed water may lead to competition for soil (sodium bentonite) binding sites. The positive statistical correlation between sodium bentonite volume and phosphorous (leaching) indicates that i) sodium bentonite represented the additional experimental source of phosphorous, and ii) increased sodium bentonite volumes resulted in significantly slower infiltration/recharge rates and thus subsurface retention times, thus permitting higher rates of subsurface leaching. Moreover, the authors consider that sediment adsorption may have been prohibited during the current study due to the relatively small experimental scale (i.e. lower migration and residence), with phosphorous removal likely to increase in concurrence with longer migration distances and residence times via increased sediment adsorption. Accordingly, larger scale field experiments are recommended for elucidation of phosphorus removal and leaching from sodium bentonite infiltration reducing treatment layers.

High COD and BOD removal efficiencies may be achieved in the vadose zone via a suite of processes including volatilization, adsorption, chemical conversion and biodegradation (Greskowiak *et al.*, 2006; Sattar *et al.*, 2016). Previous work has shown that recharging organic matter are primarily removed via biodegradation, with a comparatively small proportion also removed by adsorption (Guo & Li, 2004; Sattar *et al.*, 2016). Moreover, Pell & Nyberg (1989) have shown that organic biodegradation in the subsurface is typically more effective in aerobic conditions. In the current study, the *Re* of BOD in the infiltration-reduction layer increased in concurrence with the BC content from 27% (BM12) to 43% (BM20). Similarly, the Re of COD varied from 24% (BC12) to 45% (BC20). In both cases, a relatively high removal rate was exhibited at 200mm in the RM column. In all cases (i.e. treatment and controls), the infiltration-reducing layer and top 200mm soil depth accounted for most BOD and COD removal. For example, approximately 88% of BOD_5 removal within the BC16 column took place within the top 200mm, while over 93% of COD_{CR} removal took place within the uppermost 200mm in the same column. Accordingly, it is concluded that riverbed media exhibited a limited capacity for removal, with both BOD_5 and COD_{CR} removal shown to increase in concurrence with an increasing sodium bentonite fraction (Figures 8 & 9), due to increased adsorption capacity and hydraulic retention time. The limited BOD and COD adsorptive capacity exhibited by riverbed media likely resulted in reduced subsurface microbial degradation time, while high levels of nutrient consumption within shallow treatment layers would lead to reduced microbial loading in underlying media. Furthermore, the removal efficiency for organic pollutants was shown to decrease significantly during later experimental phases (Figures 8 & 9) due to a decreased contaminant carrying capacity, with lower temperatures during these later stages also reducing the microbial metabolic rate. However, in the absence of explicit data pertaining to microbial loading and associated subsurface processes, further work is required to elucidate these biological mechanism(s)

following infiltration reduction by a sodium bentonite treatment layer.

It is important to note that while the experimental approach adopted here comprises inherent advantages, scale effects may also occur at the meso-scale, for example, it is difficult to accurately reproduce and thus, appropriately reflect water transport (infiltration/recharge) conditions within the vadose zone (Zheng, 2006). The current study only investigated utilized on soil column depth and diameter, thus further work should seek to elucidate the effects of varying longitudinal spatial scales on subsurface decontamination processes i.e. longer subsurface residence and travel times. This is particularly the case with respect to phosphorus removal and leaching, as the authors consider that the shorter subsurface residence and migration times associated with the current experiment may have prohibited sediment adsorption.

4. Conclusions

- A 20mm layer comprised of a sodium bentonite and clay mixture (BC) was shown to effectively reduce reclaimed water infiltration, in addition to representing the primary NH_4^+-N and organic contaminant removal site during meso-scale column experiments. Contaminant removal efficiency (R_e) was shown to increase in concurrence with the sodium bentonite content of the mixture. Natural riverbed sediments exhibited no significant removal effect for NO_3^-N, BOD_5, or CODcr.
- At a 12% sodium bentonite content (BC12), the removal efficiency (R_e) of NH_4^+-N was found to be >80%, which was similar to the calculated R_e associated with a 60mm layer of natural local sediment (RM). A 20% sodium bentonite content layer was associated with approximately 97.4% NH_4^+-N removal, thus complying with current national groundwater quality standards.
- Measured removal efficiencies of BOD_5 and CODcr ranged from 37.5–55.2% and 37.8–51.5, respectively, and were positively correlated with sodium bentonite content.
- The removal effects of NO_3^-N and TN were markedly lower in treatment (BM) columns than those observed in the control (RM) column, with removal rates shown to decrease in parallel with an increasing sodium bentonite proportion. This is likely due to the presence of aerobic conditions in the BM columns, thus prohibiting denitrification.
- Significant amounts of phosphorus were leached during infiltration, with leaching was found to increase in concurrence with rising sodium bentonite contents when compared with the untreated control (CK) soil column.
- The current study provides a technical baseline for the efficacy of sodium bentonite as an

effective bi-functional material for preventing groundwater contamination prevention in areas utilizing reclaimed water. Findings indicate that sodium bentonite-clay mixes may represent a feasible alternative for managing recharge of non-potable aquifers with reclaimed wastewater.

Acknowledgments

The authors gratefully acknowledge financial support provided by the Chinese National Natural Science Fund (Grant No. 51321001), the Program for Beijing Science and Technology Plan Projects (Grant No. D090409004009004), the Ministry of Water Resources Research Special Funds for Public Welfare Industry Project (Grant No. 201001067).

References

Abel, C. D., Sharma, S. K., Mersha, S. A., & Kennedy, M. D. (2014). Influence of intermittent infiltration of primary effluent on removal of suspended solids, bulk organic matter, nitrogen and pathogens indicators in a simulated managed aquifer recharge system. *Ecological Engineering*, **64**, 100-107.

An S., Gardner WS. (2002). Dissimilatory nitrate reduction to ammonium (DNRA) as a nitrogen link, versus denitrification as a sink in a shallow estuary (Laguna Madre/Baffin Bay, Texas). *Marine Ecology Progress Series*, **237**, 41-50.

Bakandritsos A., Steriotis T., Petridis D. (2004). High surface area montmorillonite-carbon composites and derived carbons. *Chemistry of materials*, **16**(8): 1551-1559.

Baoliang ZLC. (2009). Use of Bentonite-Based Sorbents in Organic Contaminant Abatements. *Progress in Chemistry*, 2009: Z1.

Bate HK., Spaldin RF. (1998). Aquifer denitrification as interpreted from in-situ microcosm experiments. *Environ. Qual.*, **27**:174-182.

Bischel HN., Lawrence JE., Halaburka BJ., Plumlee MH., Bawazir AS., King JP., McCray JE., Resh VH., Luthy RG. (2013). Renewing Urban Streams with Recycled Water for Streamflow Augmentation: Hydrologic, Water Quality, and Ecosystem Services Management. *Environmental Engineering Science* **30**: 455–479

Chhipi-Shrestha G., Hewage K., Sadiq, R. (2017). Microbial quality of reclaimed water for urban reuses: Probabilistic risk-based investigation and recommendations. *Science of The Total Environment*, **576**, 738-751.

Dong P., Liang S., Carlton EJ., Jiang Q., Wu J., Wang L., Remais JV. (2012). Urbanisation and health in China. *Lancet*. **379**(9818):843-852

Drzyzga O., Blotevogel KH. (1997). Microbial degradation of diphenylamine under anoxic conditions. *Current microbiology*, **35**(6): 343-347.

Fierer N., Schimel JP., Holden PA. (2003). Variations in microbial community composition through two soil depth profiles. *Soil Biology and Biochemistry*, **35**(1): 167-176.

Foster SSD., Chilton PJ. (2003). Groundwater: the processes and global significance of aquifer degradation. *Phil. Trans. R. Soc.* **25:**1957–72

GB/T14848-93 Quality Standard for Groundwater. Beijing：National Standard Publishing House，1994

Greskowiak J., Prommer H., Massmann G., Nutzmann G. (2006). Modeling seasonal redox dynamics and the corresponding fate of the pharmaceutical residue phenazone during artificial recharge of groundwater. *Environ Sci. Technol.* **40**(21):6615–6621

Grischek T., Hiscock KM., Metschies T. (1998). Factors affecting denitrification during infiltration of river water into a sand and gravel aquifer in Saxony, Germany. *Water Research*, **32**(2): 450-460.

Guo W., Li PJ. (2004). Research Advances on Rapid Infiltration Land Treatment System for Wastewater. *Techniques and Equipment for Environmental Pollution Control*, **8**:1-7.

Haghseresht F., Wang S., Do DD. (2009). A novel lanthanum-modified bentonite, Phoslock, for phosphate removal from wastewaters. *Applied Clay Science.* **46**:369–375.

Hill AR., Devito KJ., Campagnolo S., Sanmugadas K. (2000). Subsurface denitrification in a forest riparian zone: interactions between hydrology and supplies of nitrate and organic carbon. *Biogeochemistry*, **51**(2), 193-223.

Huang RH., Wu YG., Yang BC. (2006). Environmental Behaviour of NH4+-N in System of Vertical River Bank Filtration. *Journal of Earth Sciences and Environment*, **28**(1): 92-95.

Idelovitch E., Icekson-Tal N., Avraham O., Michail M. (2003). The long-term performance of Soil Aquifer Treatment (SAT) for effluent reuse. *Water Science and Technology: Water Supply*, **3**(4), 239-246.

Kanarek A., Michail M. (1996). Groundwater recharge with municipal effluent: Dan region reclamation project, Israel. *Water Science and Technology*, **34**(11), 227-233.

Klika Z., Kraus L., Vopálka D. (2007). Cesium uptake from aqueous solutions by bentonite: a comparison of multicomponent sorption with ion-exchange models. *Langmuir*, **23**(3): 1227-1233.

Kopchynski T., Fox P., Alsmadi B. (1996). The effects of soil type and effluent pre-treatment on soil aquifer treatment. *Water Science and Technology*, **34**(11): 235-242.

Kumar S., Mandal A., Gurja C. (2016). Synthesis, characterization and performance studies of polysulfone and polysulfone/polymer-grafted bentonite based ultrafiltration membranes for the efficient separation of oil field oily wastewater. *Process Safety & Env. Prot*. **102**: 214-228

Lee MS., Lee K., Hyun Y. (2006). Nitrogen transformation and transport modelling in groundwater aquifers. *Ecological Modelling*, **192**(1): 143-159.

Li YK., Yang PL., Liu PB. (2012). Environmental Impact of Reclaimed water to Yongding River for Ecological Use and key Technology Study. *China Water Resources*. **5**:30-34

Liu X., Wang X. (2009). Primary Research on the self-purification of contamination in unsaturated zone. *Ground Water*, **31**(5):79-82

Lu S., Jin X., Yu G. (2006). Nitrogen removal mechanism of constructed wetland. *Acta Ecologica Sinica*, **26**(8):2670-2677

Lumbanraja J., Evangelou VP. (1994). Adsorption-desorption of potassium and ammonium at low cation concentrations in three Kentucky subsoils. *Soil Science*, **157**(5): 269-278.

O'Kane JP., Flynn D. (2007). Thresholds, switches and hysteresis in hydrology from the pedon to the catchment scale: a non-linear systems theory. *Hydrology and Earth System Sciences Discussions*, **11**(1), 443-459.

Pell M., Nyberg F. (1989). Infiltration of wastewater in a newly started pilot sand-filter system: I. Reduction of organic matter and phosphorus. *Journal of Environmental Quality*, **18**(4): 451-457.

Puckett LJ., Cowdery TK. (2002). Transport and fate of nitrate in a glacial outwash aquifer in relation to ground water age, land use practices, and redox processes. *Journal of Environmental Quality*, **31**(3): 782-796.

Putra EK., Pranowo R, Sunarso J, Indraswati N, Ismadji S. (2009). Performance of activated carbon and bentonite for adsorption of amoxicillin from wastewater: Mechanisms, isotherms and kinetics. *Water Research.* **43**:2419–2430.

Rauch-Williams T., Drewes JE. (2006). Using soil biomass as an indicator for the biological removal of

effluent-derived organic carbon during soil infiltration. *Water Research*, **40**(5): 961-968.

Richards S., Withers P.J., Paterson E., McRoberts CW., Stutter M. (2017). Removal and attenuation of sewage effluent combined tracer signals of phosphorus, caffeine and saccharin in soil. *Environmental Pollution*. In Press

Rose JB. (2007). Water reclamation, reuse and public health. *Water Sci. Tech*. **55**:275-282

Sattar AM. (2016). Prediction of organic micropollutant removal in soil aquifer treatment system using GEP. *Journal of Hydrologic Engineering*, **21**(9), 04016027.

Shi LN., Lin YM., Zhang X., Chen ZL. (2011). Synthesis, characterization and kinetics of bentonite supported nZVI for the removal of Cr (VI) from aqueous solution. *Chem. Eng. Jour.* **171**(2):612–617

Shuang X. (2008). Removals of dissolved organic matter in secondary effluents by soil-aquifer treatment techniques. Unpublished PhD Thesis, Harbin Institute of Technology, 2008.

Starr RC., Gillham RW. (1989). Controls on denitrification in shallow unconfined aquifers. Contaminant Transport in Groundwater. Kobus & Kinzelbach (Eds), Rotterdam. 1989 Apr 4:51-6.

Valazquez DJ. (2016). Soil Aquifer Treatment for wastewater reclamation in a high water demand society. Unpublished PhD Thesis. University of Western Ontario. Canada. September 2016

Vanderzalm JL., Page DW., Barry KE., Dillon PJ. (2013). Application of a probabilistic modelling approach for evaluation of nitrogen, phosphorus and organic carbon removal efficiency during four successive cycles of aquifer storage and recovery (ASR) in an anoxic carbonate aquifer. *Water Research*, **47**(7), 2177-2189.

Wu W. (2009). Research on groundwater vulnerability experiment of reclaimed wastewater district and irrigation allocation. Unpublished PhD Thesis, China Geosci. Univ. Beijing

Yu Z., Yuan X., Liu S. (2011). Effect of hydraulic conditions on treatment of polluted river water by hybrid constructed wetlands. *Chinese Journal Environmental Engineering*, **5**(04):757-762

Zhang Z., Jia P. (2010). Eco-role of ecological anti-seepage technology of Sodium bentonite in urban river harnessing. *Water Resources and Hydropower Engineering*, **3**:005.

Zheng YX. (2006). Experimental Study on Infiltration System for Slightly-Polluted Surface Water Treatment. Unpublished PhD Thesis. Beijing: China Agricultural University

Zhou C., Fan X., Ning Z., Li P., Liu C., Yang P., Li Y. (2015). Reducing riverbed infiltration using mixtures of sodium bentonite and clay. *Environmental Earth Sciences*, **74**(4), 3089-3098.

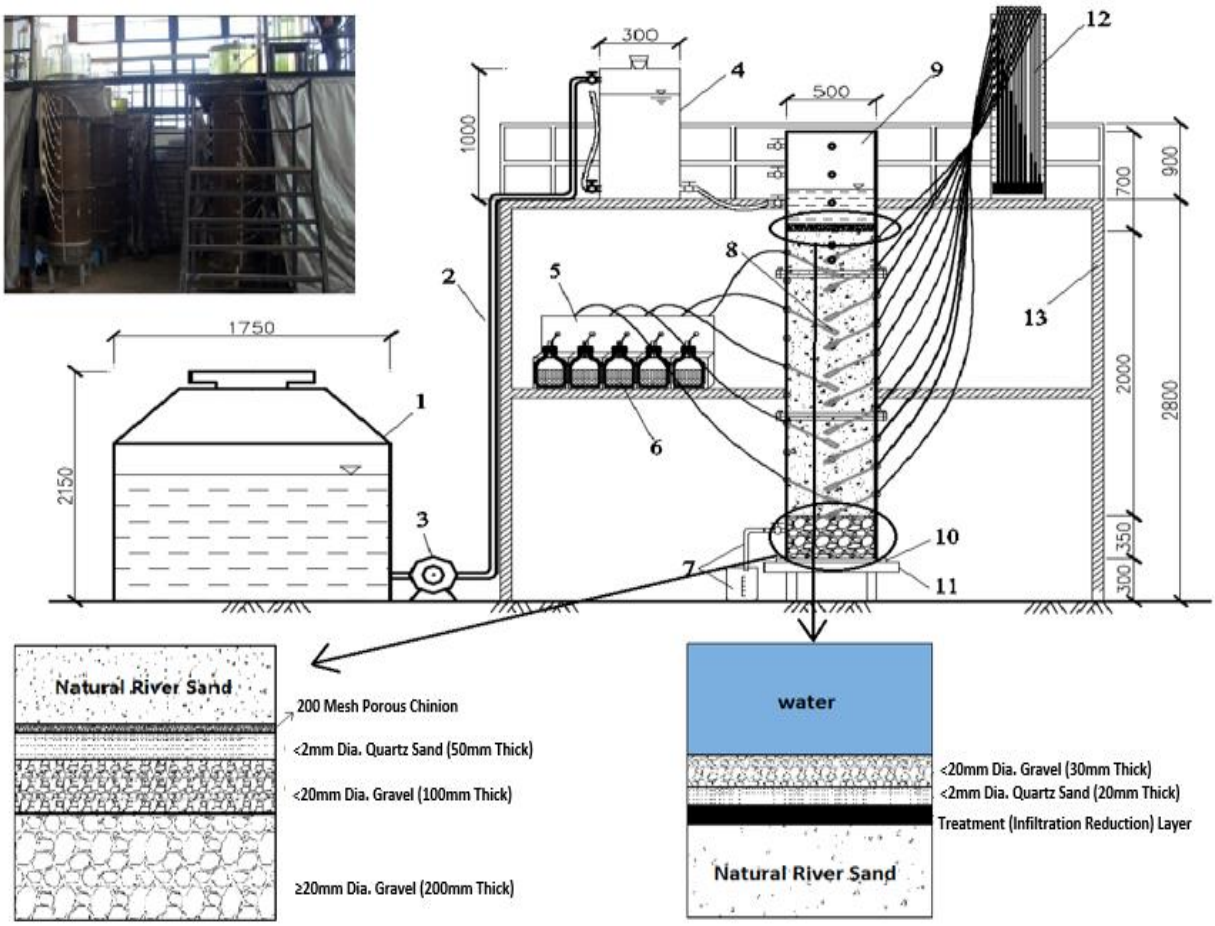

Figure 1. (a) Schematic of experimental soil columns with inset photograph of laboratory setup used in the current study (All units in mm); 1- storage tank, 2- PVC pipeline for water supplying, 3-water pump, 4-Mariotte bottle, 5-PVC protection box, 6- soil water sample bottle, 7- groundwater collector, 8- porous clay pipe, 9 plexiglass soil column, 10- rubber washer, 11- steel supporting base, 12-tensiometer, 13- steel supporting frame; (b) Structural composition of simulation column filling

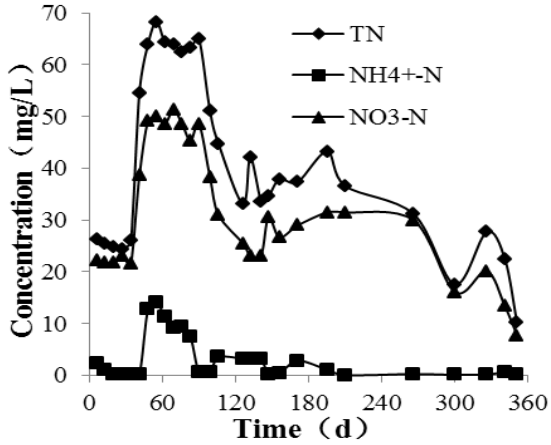

(a) Nitrogen (TN, NO_3-N, NH_4-N)

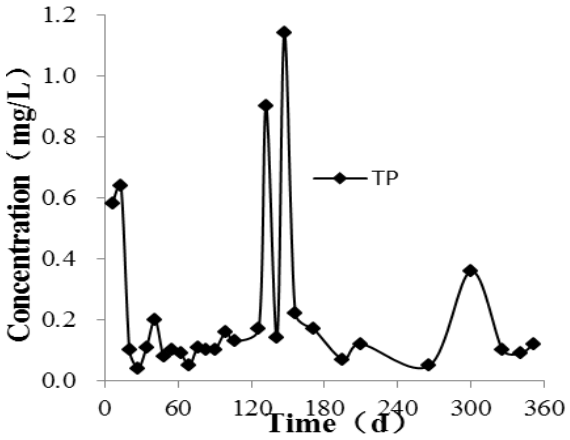

(b) Total Phosphorous

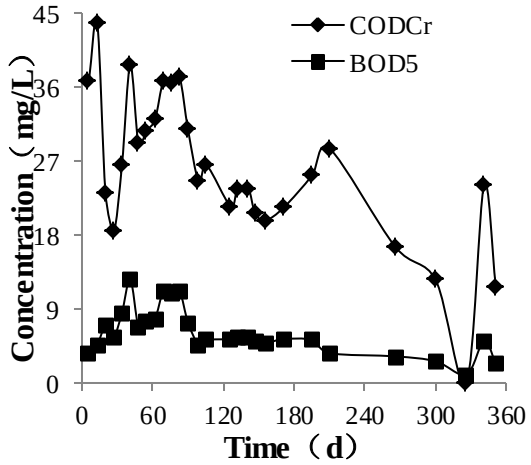

(c) Organic Contaminant Indicators

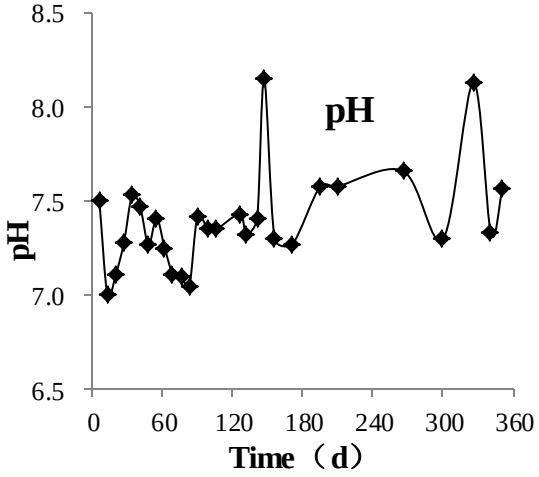

(d) pH

Figure 2. Pre-experimental reclaimed water quality

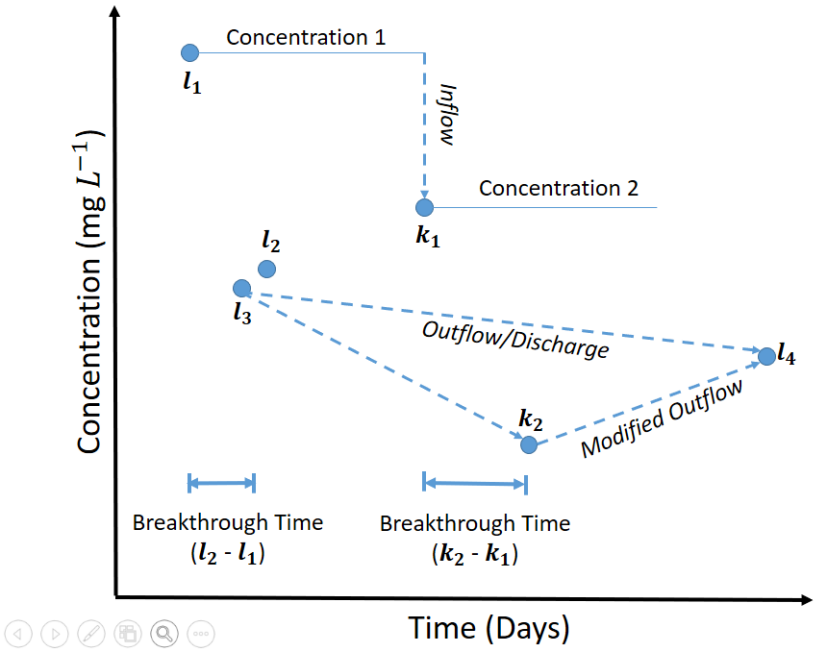

Figure 3. Schematic outlining aqueous-phase concentration calculations

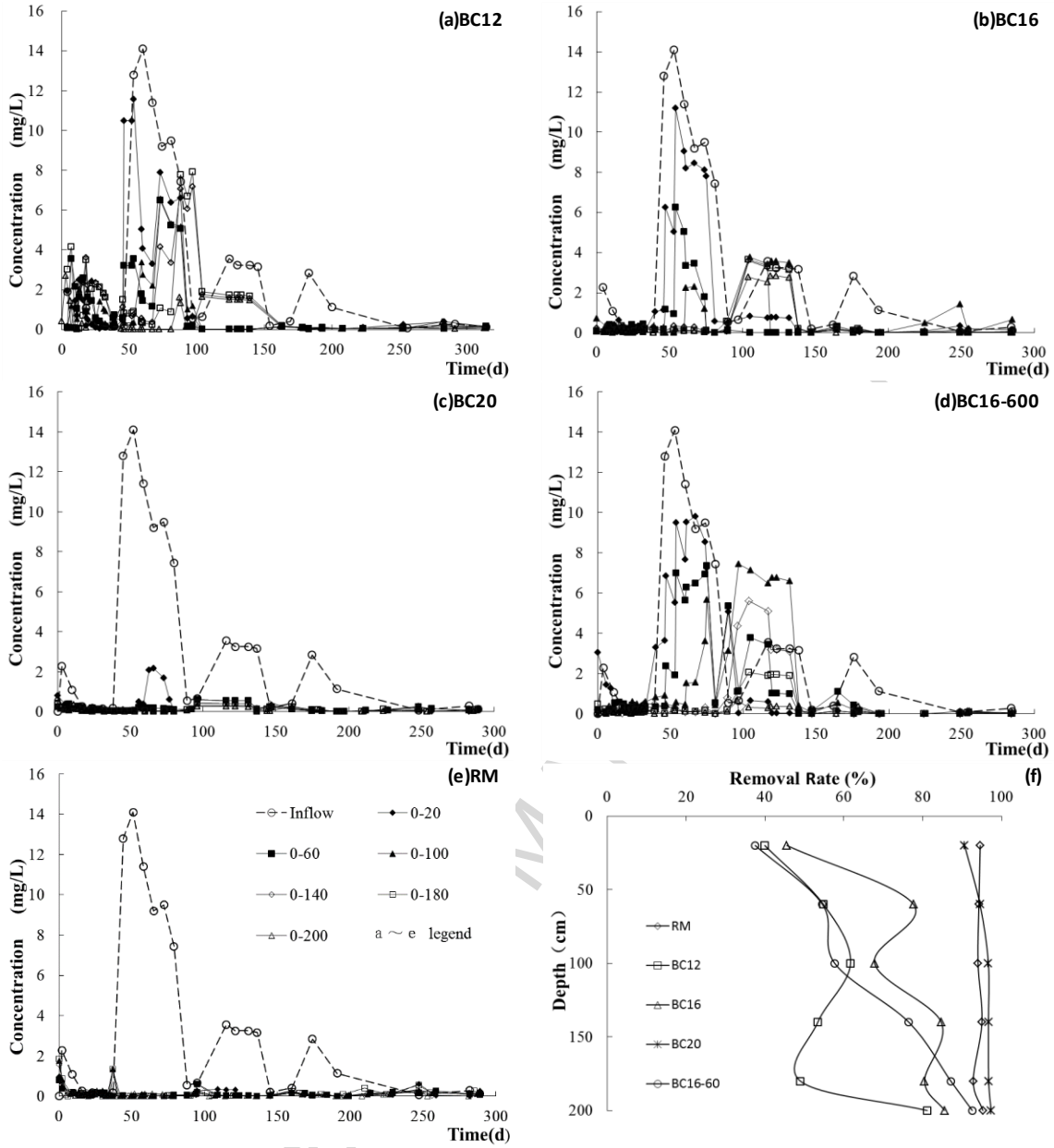

Figure 4. Measured NH_4^+-N concentration in experimental (a-c) and control (d-e) mesoscale columns, and calculated R_e for all groups (f)

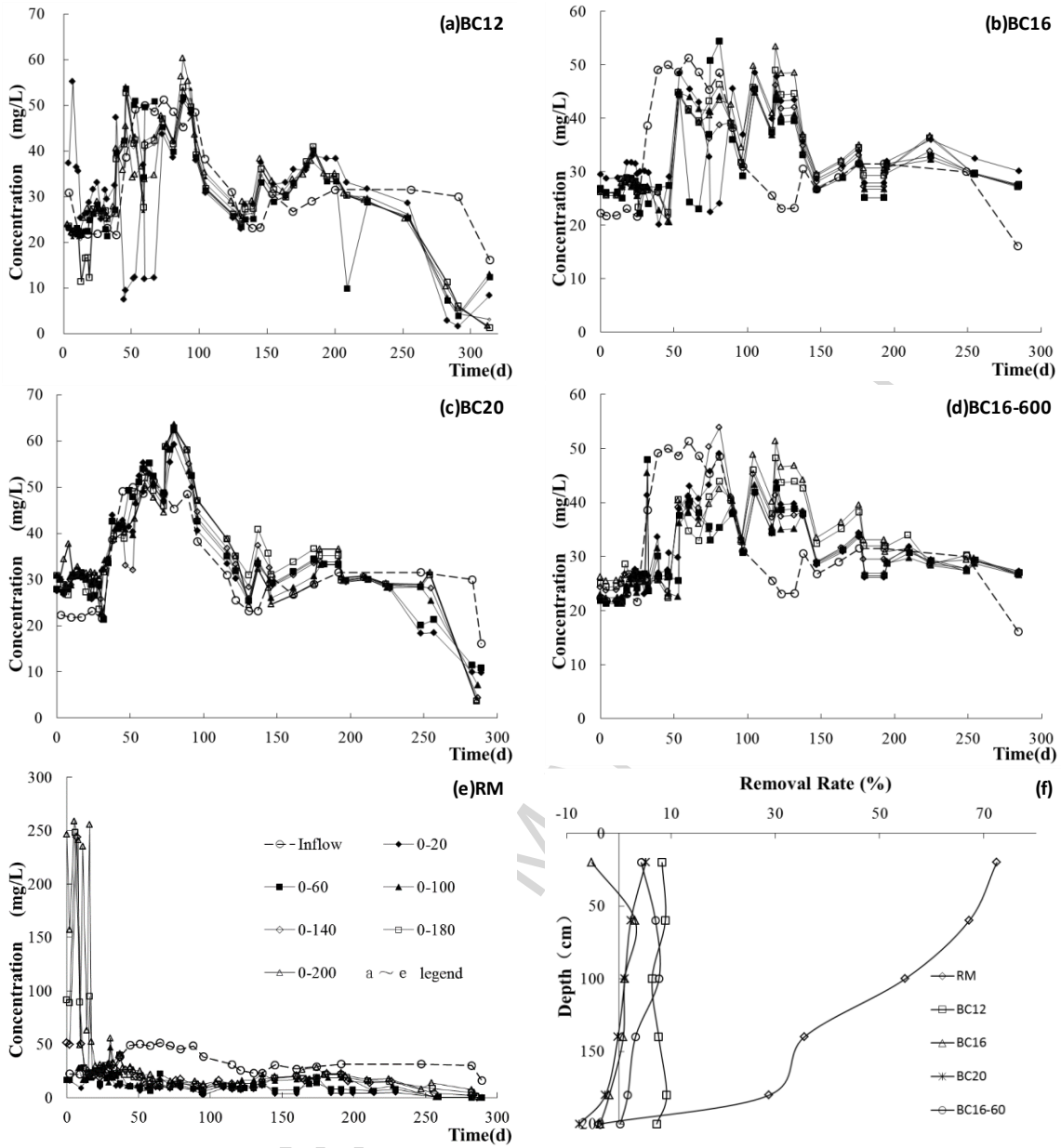

Figure 5. Measured NO_3^-N concentration in experimental (a-c) and control (d-e) mesoscale columns, and calculated R_e for all groups (f)

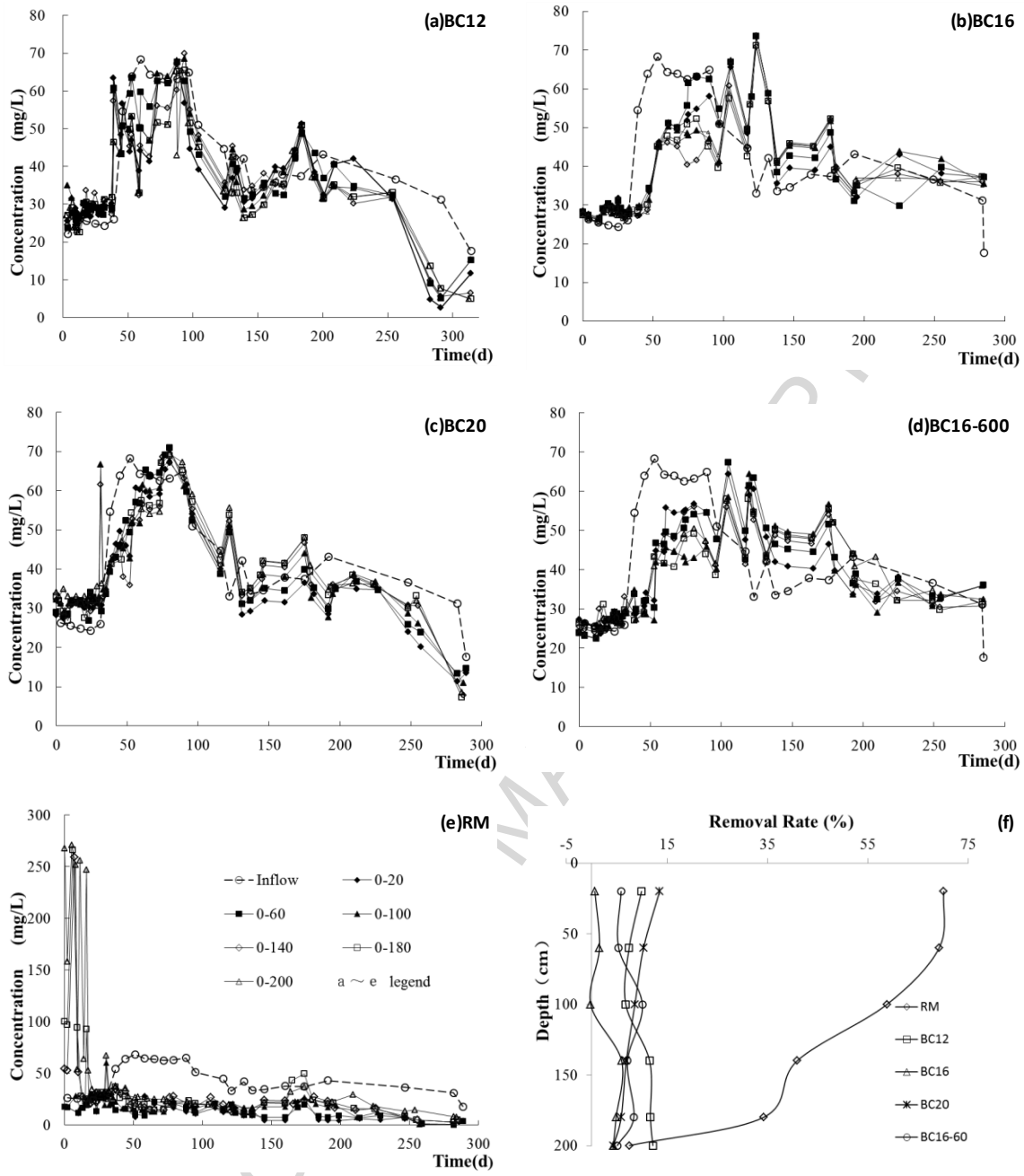

Figure 6. Measured Total Nitrogen (TN) concentration in experimental (a-c) and control (d-e) mesoscale columns, and calculated R_e for all groups (f)

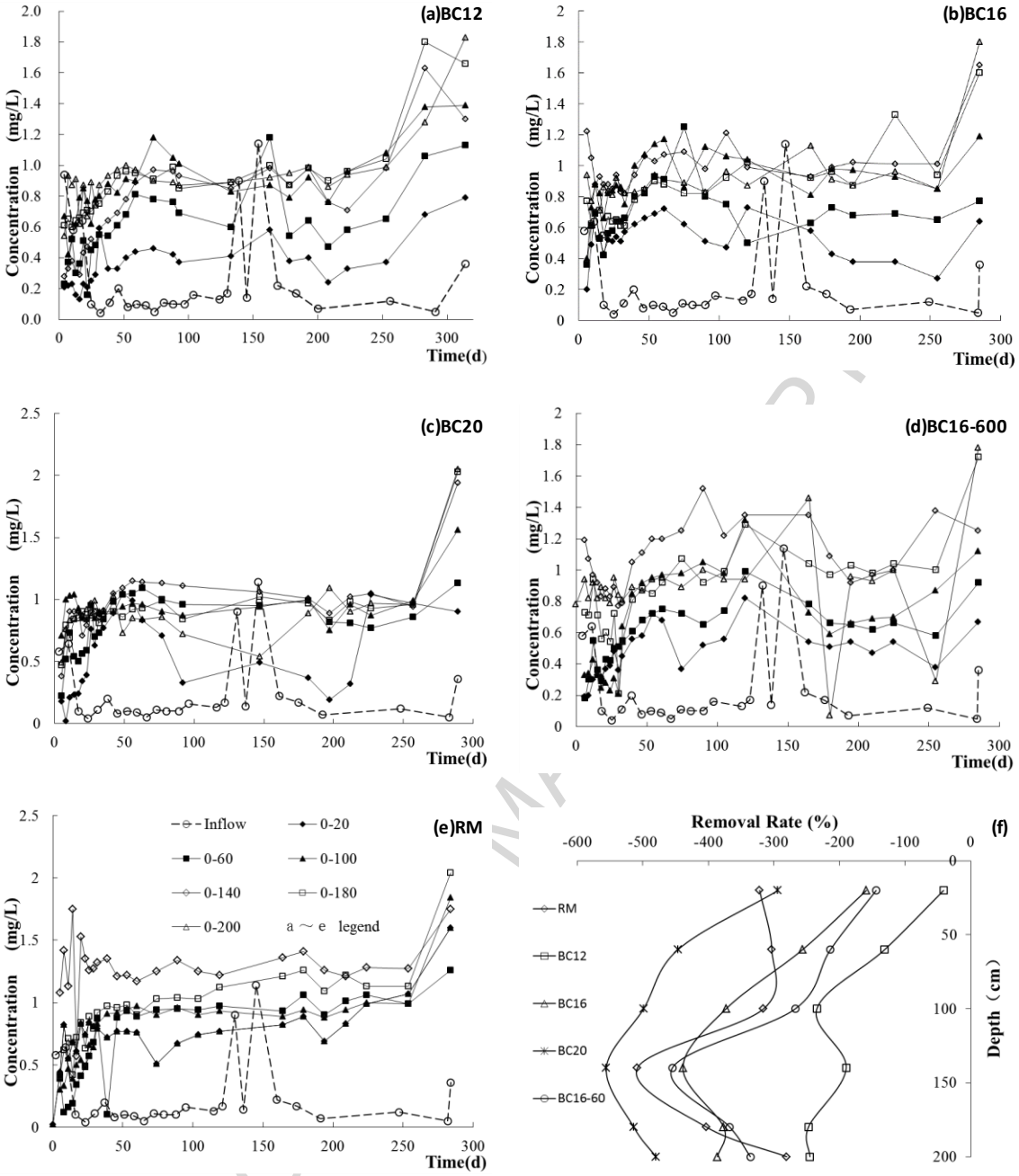

Figure 7. Measured Total Phosphorous (TP) concentration in experimental (a-c) and control (d-e) mesoscale columns, and calculated R_e for all groups (f)

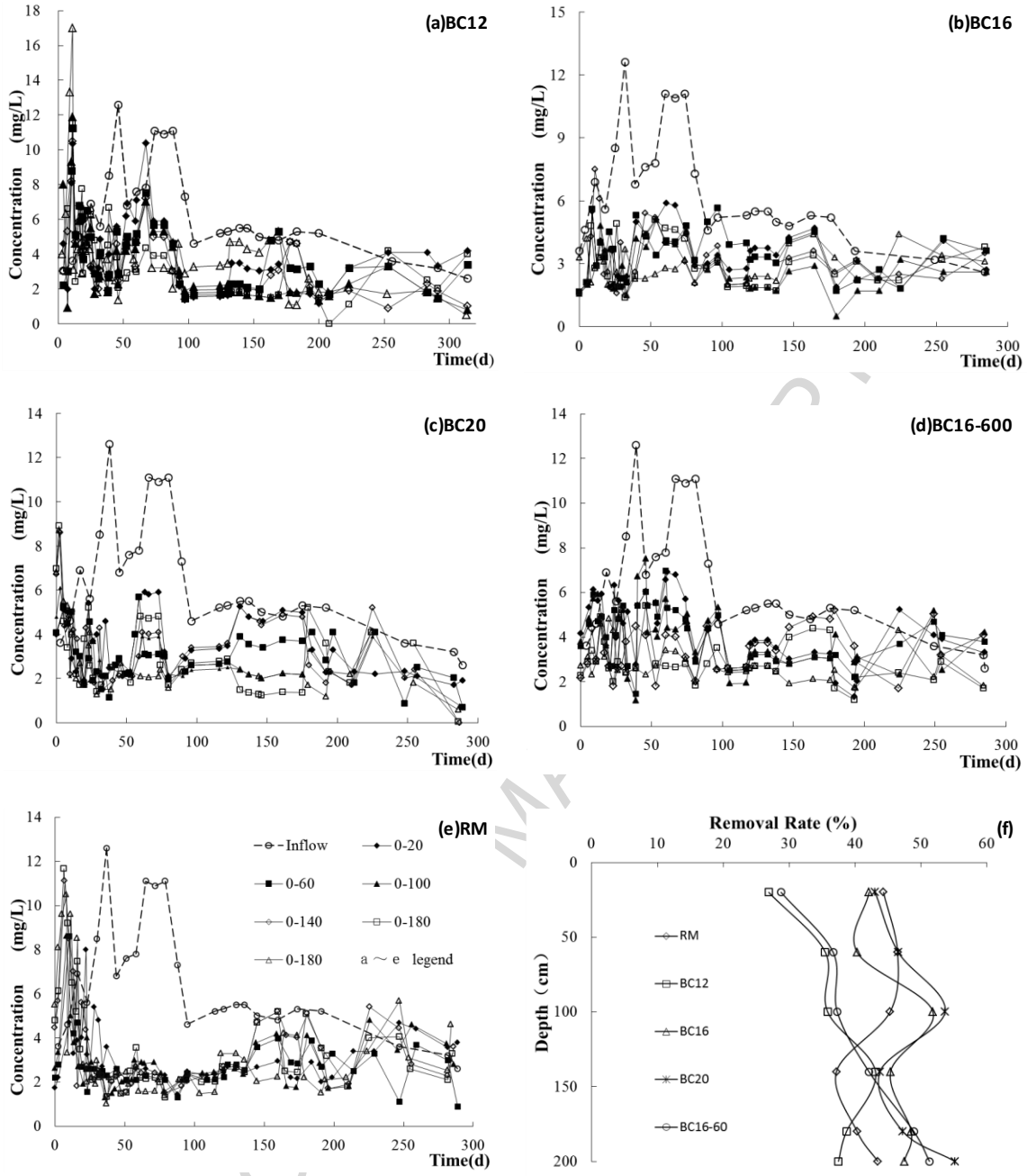

Figure 8. Measured BOD_5 concentration in experimental (a-c) and control (d-e) mesoscale columns, and calculated R_e for all groups (f)

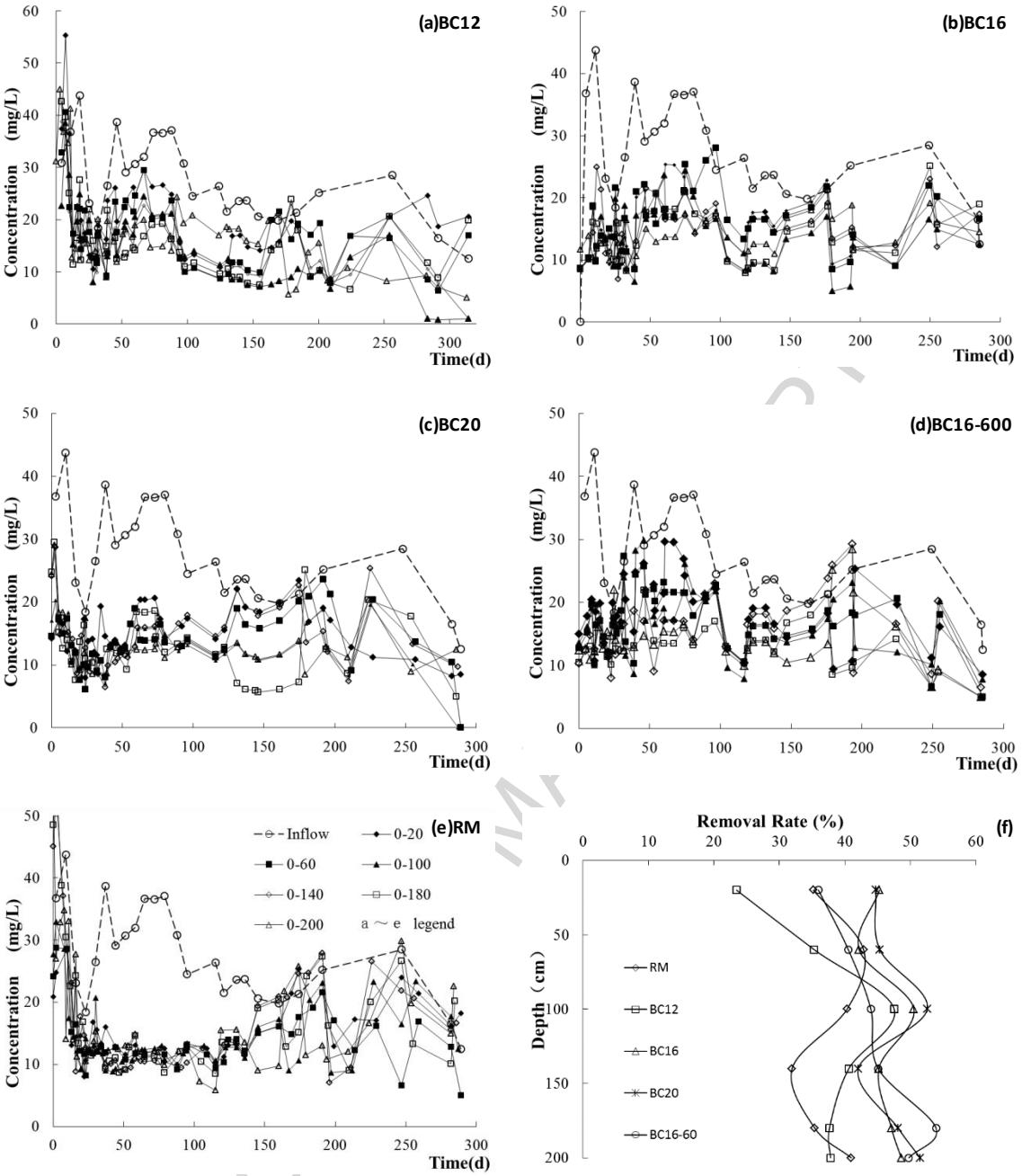

Figure 9. Measured CODcr concentration in experimental (a-c) and control (d-e) mesoscale columns, and calculated R_e for all groups (f)

Table 1. Summary of experimental and control treatments including associated materials, experimental setup, filtrate and operational head

Soil Column	Test Material	Column Media	Filtrate	Head (mm)
CK	None	2000mm Undisturbed Riverbed Soils (URS)	Deionized Water	300
BC16-600	16% Sodium bentonite	50mm filter layer + 20mm BC16 + 2000mm URS	Reclaimed Water	600
RM	Natural (local) river mud	50mm filter layer + 60mm RM + 2000mm URS	Reclaimed Water	300
BC12	12% Sodium bentonite	50mm filter layer + 20mm BC12 + 2000mm URS	Reclaimed Water	300
BC16	16% Sodium bentonite	50mm filter layer + 20mm BC16 + 2000mm URS	Reclaimed Water	300
BC20	20% Sodium bentonite	50mm filter layer + 20mm BC20 + 2000mm URS	Reclaimed Water	300

Table 2. Initial measured contaminant quantities in natural river mud

pH	Ammonium	Available P	TN	TP	Organic	TOC	CEC	EC
	mg/kg	mg/kg	g/kg	g/kg	g/kg	g/kg	mmoL/kg	µs/cm
7.68	50.8	107	4.16	1.51	83.4	48.4	174	31.4

Note: TN – Total Nitrogen; TP – Total Phosphorous; TOC – Total Organic Carbon; CEC – Cation Exchange Capacity; EC – Electrical Conductivity

Table 3. Primary physical characteristic of experimental materials

Material	Particle Size Distribution (%)					Dry Weight (g/cm^3)	Initial Moisture Content (%)
	Coarse	Medium	Fine	Super Fine	Coarse Silt		
Riverbed Media	8.6	37.3	24.2	22.8	7.1	2.1	4.0
River Mud	7.5	28.1	30.4	16.0	14.0	1.2	158.9
Bentonite	0.5	2.6	18.9	15.0	63.0	0.8	12.0
Clay	-	2.5	10.5	63.0	24.0	1.8	16.7

Note: Coarse: 2.0-0.5mm; Medium: 0.5-0.25mm; Fine: 0.1-0.05mm; Super Fine: 0.1-0.05mm; Coarse Silt: <0.05mm

Table 4. Background contaminant values associated with filtrate from undisturbed riverbed soils (CK). All values reported in mg/L

Leaching time	TN	Ammonium	Nitrate-N	TP	CODcr	BOD_5
0h	124	0.43	115	0.33	32.9	10.2
3h	2.21	ND	1.94	0.72	9.67	1.9
10h	1.91	ND	1.61	0.78	8.02	1.8
15h	1.7	ND	1.39	0.75	ND	0.8
20h	1.57	ND	1.27	0.76	ND	0.7

Note: ND – Non-detect; CODcr Detection Limit = 5.0mg/L; NH_4N Detection Limit = 0.02mg/L

Table 5. Analytical laboratory methods and detection limits

Analyte	Method	Standard	MDL (mg/L)	LDL (mg/L)	UDL (mg/L)	RSD (%)
CODcr	Fast digestion-spectrophotometric method	HJ/T 399-2007	2	15	1000	2.9
BOD_5	Dilution and seeding method	HJ 505-2009	0.5	2	6000	3.6
TP	Molybdate method	GB11893-89	0.01	0.05	0.6	1.4

TN	Alkaline potassium persulfate digestion UV spectrophotometry	HJ 636-2012	0.05	0.2	7	5
NH_4^+-N	Nessler's reagent spectrophotometry	HJ 537-200	0.025	0.1	2	2.5
NO_3^-N	Ultraviolet spectrophotometry	HJ/T 346–2007	0.08	0.32	4	2.6

Note: MDL – Method Detection Limit; LDL – Lower Determination Limit; UDL – Upper Determination Limit; RSD – Relative Standard Deviation

Table 6. Pre-experimental contaminant concentrations measured from solid phase experimental media

Media Type	TN (g/kg)	TP (g/kg)	NH_4^+-N (mg/kg)	NO_3^-N (mg/kg)
Riverbed media	0.36	0.34	None（<1.25）	3.46
Natural sediment	4.16	1.51	50.8	-
Sodium bentonite	0	0	0	0

Table 7. Solid phase contaminant concentration associated with experimental media at varying depths after one year of recycled water infiltration

Media Type	Contaminant	Infiltration-reducing layer		Riverbed media (mm)				
		Surface layer	Bottom layer	0	200	600	1200	2000
RM	TN	2.80	3.02	0.32	0.31	0.30	0.28	0.38
	TP	1.48	1.67	0.61	0.63	0.67	0.66	0.76
	NH_4^+-N	6.49	62.8	0.41	0.55	0.43	0.75	0.39
	NO_3^-N	32.7	28.9	7.59	7.75	8.21	8.89	7.89
BC12	TN	0.63	0.56	0.34	0.30	0.35	0.32	0.39
	TP	0.39	0.38	0.50	0.57	0.69	0.70	0.64
	NH_4^+-N	1.33	0.56	0.26	0.39	0.81	0.52	0.14
	NO_3^-N	17.3	8.48	8.69	6.59	8.42	6.72	6.55
BC16	TN	0.66	0.57	0.35	0.35	0.33	0.30	0.35
	TP	0.38	0.36	0.49	0.55	0.60	0.69	0.74
	NH_4^+-N	0.67	0.42	0.28	0.32	0.44	0.77	0.92
	NO_3^-N	11.4	9.84	6.99	6.53	6.50	5.29	6.58

BC16-600	TN	0.75	0.59	0.48	0.35	0.33	0.35	0.40
	TP	0.36	0.32	0.65	0.62	0.62	0.74	0.63
	NH_4^+-N	6.11	0.73	1.23	0.2	0.6	0.22	1.08
	NO_3^-N	16.2	8.96	10.5	7.66	7.59	7.44	11.2
BC20	TN	0.60	0.54	0.34	0.35	0.24	0.26	0.34
	TP	0.38	0.38	0.63	0.60	0.59	0.72	0.72
	NH_4^+-N	0.65	0.72	0.23	0.26	0.52	0.10	1.08
	NO_3^-N	12.3	4.69	7.63	6.48	5.98	6.48	7.48

Note: TN (g/kg); TP (g/kg); NH_4^+-N (mg/kg); NO_3^-N (mg/kg)

Highlights

- Mesoscale soil columns used to simulate soil aquifer treatment system
- BC reduced wastewater infiltration by 30-150 times natural rate
- High rates of BOD_5, COD_{cr}, and NH_4^+-N removal by BC
- Low rates of NO_3-N removal exhibited, with active P leaching
- BC may be an effective bi-functional material for SAT in high permeability regions